

## Quantum Interference Effects in Inelastic Electron-Photon Scattering in a 2D Ballistic Microstructure

L. Y. Gorelik,\* Anna Grincwajg, V. Z. Kleiner,† R. I. Shekhter, and M. Jonson

Department of Applied Physics, Chalmers University of Technology and Göteborg University, S-412 96 Göteborg, Sweden  
(Received 22 March 1994)

We demonstrate a new effect where the electron-photon interaction in a ballistic microconstriction plays the same role as impurity scattering does in a “dirty” system. In the presence of an external electromagnetic field all relevant photons are coherent, and spatial interference effects in electron-photon scattering become possible in spite of the inelastic nature of the collisions. These interference effects can be controlled by the gate voltage or the frequency of the electromagnetic field. As an illustration we calculate the photoconductance of a double point-contact geometry.

PACS numbers: 73.20.Dx, 73.40.Gk

Quantum interference effects in impurity scattering of electrons and the associated spatial localization of electrons has attracted much interest during recent years [1]. Electron localization is the result of phase coherent multiple scattering in a system of randomly distributed impurities and is a prominent effect in highly disordered systems. In this Letter we consider a new type of effect where electron-photon scattering in a *ballistic* system plays the same role as impurity scattering does in a “dirty” system.

The system we consider is a 2D ballistic microstructure subject to a homogeneous electromagnetic field. The microstructure is fabricated by putting a split gate configuration on top of a GaAs heterostructure, thereby creating a narrow constriction in the two-dimensional electron gas [2]. The geometry of the microstructure depends on the shape of the gate. A simple example of an adiabatic microstructure geometry is shown in Fig. 1(a). The electromagnetic field, polarized in the  $y$  direction, induces transitions between different transverse energy states (modes) in the system. Fig. 1(b) shows the transverse energies for different modes, as a function of  $x$ . For a transition to occur, the energy quantum  $\hbar\omega$ , where  $\omega$  is the frequency of the

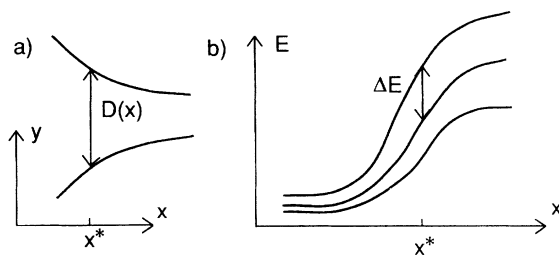


FIG. 1. (a) Simple example of an adiabatic microconstriction geometry with varying width  $D(x)$ . An electromagnetic field, polarized in the  $y$  direction, induces transitions between different transverse energy states. (b) The corresponding set of transverse energies as a function of  $x$ . A transition is possible when  $\Delta E(x) = \hbar\omega$  where  $\Delta E$  is the difference between two transverse energies. In this particular geometry there exists only one point  $x^*$  where this condition is fulfilled.

field, must correspond to the difference  $\Delta E$  between two transverse energies. For a certain  $\hbar\omega$  there exists—in the geometry of Fig. 1(a)—only one point  $x^*$  where such a transition is possible, since  $\Delta E$  depends on  $x$ . Thus the electron-photon interaction is localized to a point in space in the same way as impurity scattering is.

A more general geometry is shown in Fig. 2. In this case there exists a number of points  $x_i^*$  satisfying  $\Delta E(x_i^*) = \hbar\omega$ . The situation corresponds to a channel with a number of localized scattering centers. The position of the scattering centers can be changed by varying the frequency  $\omega$  or the gate voltage.

The analogy to impurity scattering becomes even clearer when noting that in a microconstriction electron-photon interaction can result in backscattering. This happens when there is a transition between a propagating and a nonpropagating mode. A mode is propagating when its total energy is larger than its maximum transverse energy, otherwise it is reflected by the constriction and the photon induces backscattering of electrons in the microconstriction; the resulting photoconductance oscillations have been studied elsewhere [3] by us.

There is, however, an important difference between impurity scattering and this type of electron-photon scattering; the impurity scattering is elastic but the electron-photon scattering is inelastic. It is well known that inelastic scattering destroys the phase memory and makes

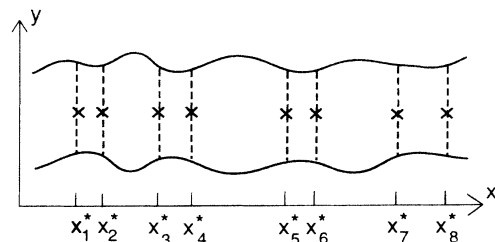


FIG. 2. An adiabatic microconstriction geometry of arbitrary shape. For this type of geometry there exists a number of points  $x_i^*$  where a photon induced intermode transition can occur. The situation corresponds to a channel with a number of localized scattering centers.

quantum interference effects impossible [1]. In our case, however, the electron-photon scattering does not lead to phase memory loss. The reason is that our source of inelastic scattering, a classical electromagnetic field, corresponds to a coherent photon state with one single phase. Therefore the electrons do not couple to a large number of degrees of freedom and their phase memory is preserved. Interference effects are therefore certainly possible in our system, even though the scattering is inelastic.

We will now illustrate such an interference effect in a simple case. Consider an adiabatic geometry with a widening, a "microwidening," see the inset of Fig. 3. The corresponding transverse energy will here (for each mode) take the shape of a well which creates bound states in the wide region. We want to investigate how the electric current through the microwidening is affected by the presence of an electromagnetic field. Only such transitions that change the current interest us, i.e., transitions between propagating and nonpropagating (bound) states. Clearly the photocurrent will be governed by the matrix element for these transitions,

$$A_{\alpha\beta} = -\frac{ieE}{m^*\omega} \langle \alpha | p_y | \beta \rangle. \quad (1)$$

Here  $E$  is the amplitude of the electromagnetic field,  $\hat{p}_y$  is the  $y$  component of the electron momentum operator, while  $e$  and  $m^*$  are the electron charge and effective mass. The electronic states  $|\alpha\rangle$  and  $|\beta\rangle$  represent a propagating and a bound state, respectively. The states are characterized by the discrete mode numbers  $n$  and  $m$ , respectively. Further, the propagating state  $|\alpha\rangle$  is

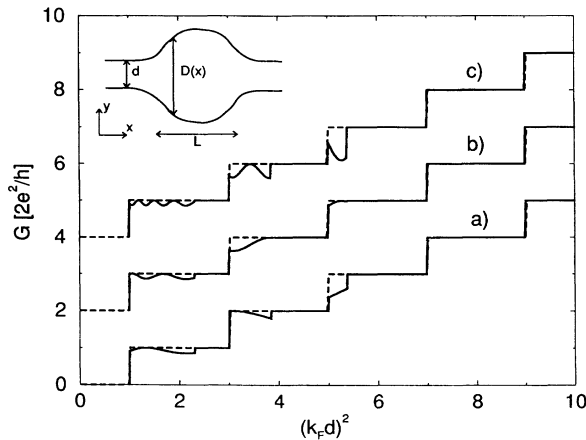


FIG. 3. Conductance as a function of the dimensionless parameter  $(k_F d)^2$  for the geometry shown in the inset. The width of the microwidening scales with  $d$ , the narrowest microstructure width. It is clearly seen how the sharp steps (dotted line) transform into an oscillatory structure when an electromagnetic field is turned on (solid line). The frequency of the field is  $1.3 \times 10^{12} \text{ s}^{-1}$ . The three graphs—vertically offset for clarity—correspond to different choices of microwidening length  $L$  and electromagnetic field amplitude  $E$ : (a)  $L = 1 \mu\text{m}$ ,  $E = E_0$ , (b)  $L = 2 \mu\text{m}$ ,  $E = E_0/2^{1/2}$ , (c)  $L = 4 \mu\text{m}$ ,  $E = E_0/2$ , where  $E_0 = 300 \text{ V/cm}$ .

characterized by the continuous longitudinal wave vector  $\pm k$  while the bound state  $|\beta\rangle$  is characterized by the discrete wave vector  $k_m$ . The corresponding adiabatic wave functions are

$$\Psi_\alpha(x) = \sqrt{\frac{k_n(-\infty)}{k_n(x)}} \exp\left(\pm i \int^x dx' k_n(x')\right), \quad (2)$$

$$\Psi_\beta(x) = \sqrt{\frac{4m^*}{\hbar T_m k_m(x)}} \sin\left(\int_{x_m}^x dx' k_m(x')\right), \quad (3)$$

where  $x_m$  is the turning point and  $T_m$  is one time period of motion for the bound state. For the propagating state the total energy  $E_\alpha$  is a continuous variable, while the total energy  $E_\beta$  for the bound state takes discrete values. However, if we consider bound states with sufficiently high energy, the energy spectrum is very dense and can be approximated by a continuum.

In the calculation of the matrix element (1) we use the stationary phase approximation [4], which is applicable when the shape of the microstructure is adiabatically smooth on the scale of the Fermi wave length. Because of the symmetry in our geometry we have two stationary points  $x^*$  and  $-x^*$  which both contribute to the integral. These two contributions correspond to two different electron trajectories, where the electron is scattered by a photon at either  $x^*$  or  $-x^*$ . The corresponding probability amplitudes will differ in phase, and their sum gives the total amplitude. The interference between the two contributions gives rise to oscillations in the matrix element. Taking the laterally confining potential to be of the parabolic type [5], the matrix element (1) is found to be

$$A_{\alpha\beta} = -\frac{ieE}{2m^*\omega} \mathcal{M}_{nm} (e^{-i\phi} + e^{i\phi}), \quad (4)$$

$$\mathcal{M}_{nm} = e^{i\varphi} \sqrt{\frac{\pi \hbar m^* k_n(-\infty)}{2 T_m k_n(x^*)}} \sqrt{\left| \frac{D(x^*)}{D'(x^*)} \right|} \sqrt{n+1} \delta_{m,n+1}, \quad (5)$$

where  $D(x)$  is the width of the microstructure,  $e^{i\varphi}$  is an overall phase factor, and the interference phase  $\phi$  can be written as

$$\phi = \frac{1}{2} \int_{-x^*}^{x^*} dx [k_n(x) - k_m(x)]. \quad (6)$$

The interference occurs because there are two possible trajectories for an electron in mode  $n$  being scattered to mode  $m$ . The phase  $\phi$  expresses the phase difference between the two trajectories, and it depends on the frequency  $\omega$  and the microstructure width.

The shape of the laterally confining potential is not particularly important. We would have gotten essentially the same result if we, in the above calculation, had used a different type of potential, like a square-box potential.

Our next step is to calculate the current in order to demonstrate how the interference oscillations show up in the photoconductance [6]. We formulate the problem as a

set of kinetic equations for the electron population in each mode [3]. The electron-photon scattering enters in a collision term that mixes the populations in different modes. Only transitions between propagating and nonpropagating states influence the photocurrent; there are two types of such transitions: (i) propagating to bound state and (ii) bound to propagating state. While weak electron-photon scattering results in small deviations from equilibrium within the propagating modes, it leads to a strong nonequilibrium population of the bound states. Hence this part of the problem has to be treated nonperturbatively. A balance equation, which ensures the time independence of the total number of electrons in the bound states, was derived and solved in the limit of small bias voltage. The conductance, which in principle depends on the population of both propagating and bound states, can then be expressed in terms of the population of the propagating states only. Hence we get the following simple-looking result for the zero bias conductance [7]

$$G = e^2 \sum_{\alpha} \frac{\partial f_{\alpha}^0}{\partial \mu} \left[ v_{\alpha} - \frac{\pi}{\hbar} \sum_{\beta} |A_{\alpha\beta}|^2 \delta(E_{\beta} - E_{\alpha} - \hbar\omega) \right]. \quad (7)$$

(Details of the calculation will be published elsewhere [8].) The first term is the ordinary quantized conductance which is independent of the electromagnetic field. The second term is the photoconductance, and it is proportional to  $|A_{\alpha\beta}|^2$ . Inserting our expression (4) for the matrix element, taking  $f_{\alpha}^0$  to be the equilibrium Fermi distribution function at zero temperature, and introducing the dimensionless frequency  $\Omega = \hbar\omega/E_F$ , the photoconductance is found to be:

$$G^{ph} = -\frac{2e^2}{h} \left( \frac{eE}{\hbar\omega} \right)^2 \frac{\pi}{8} \times \sum_n (n+1) \frac{\Theta[1 - \Omega(n + \frac{1}{2})]}{k_n(x^*)} \left| \frac{D(x^*)}{D'(x^*)} \right| \frac{(1 + \cos 2\phi)}{2} \times \Theta[k_F^2 d^2 - (2n+1)] \Theta[2n+3 - k_F^2 d^2 (1 + \Omega)], \quad (8)$$

where  $k_n(x^*) = k_F [1 - \Omega(n + 1/2)]^{1/2}$ . The step function  $\Theta[1 - \Omega(n + 1/2)]$  expresses the condition that the stationary point  $x^*$  must be in the classically allowed region for the electrons, a condition imposed by the existence of turning points. The other two step functions express the conditions that mode  $n$  (the initial state) must be propagating and mode  $n+1$  (the final state) must be nonpropagating. In the wide part of the microstructure the width  $D(x)$  is taken to be

$$D(x) = d \left( \frac{1 + \eta}{1 + \eta(2x/L)^2} \right), \quad (9)$$

where  $L$  is the length of the wide area,  $d$  is the smallest width, and  $d(1 + \eta)$  is the largest width of the microstructure, see Fig. 3. Since the energy quantum  $\hbar\omega$

must correspond to the energy difference  $\Delta E$  between the transverse states, there is a restriction on the frequency  $\omega$ . The smallest  $\Delta E$ , corresponding to the widest part of the geometry, and the largest  $\Delta E$ , corresponding to the narrowest part of the geometry, set lower and upper limits on the frequency:

$$\frac{2}{(k_F d)^2 (1 + \eta)^2} < \Omega < \frac{2}{(k_F d)^2}. \quad (10)$$

Now we will present the results of a numerical evaluation of the photoconductance, Eq. (8). The parameters used have been taken as follows: the Fermi temperature  $T_F = 200$  K, the dimensionless frequency  $\Omega = 0.3$  which corresponds to  $\omega = 1.3 \times 10^{12} \text{ s}^{-1}$ , and the geometry parameter  $\eta = 4$ . In Fig. 3 the total conductance (solid line) is shown as a function of microstructure width for three different electromagnetic field amplitudes and microwidening lengths: (a)  $L = 1 \mu\text{m}, E = E_0$ , (b)  $L = 2 \mu\text{m}, E = E_0/\sqrt{2}$ , (c)  $L = 4 \mu\text{m}, E = E_0/2$ , where  $E_0 = 300 \text{ V/cm}$ . The power of the electromagnetic field  $E_0$  in a volume  $V = 10^{-6} \text{ cm}^3$  is 0.2 W. The dotted line shows the conductance in the absence of any electromagnetic field. It is clearly seen that the sharp steps transform into an oscillatory structure when an electromagnetic field is turned on. A comparison of (a), (b), and (c) shows that the oscillations become more rapid as the length of the microstructure increases and that the field strength required to observe the effect decreases with increasing microstructure length. The oscillations are very similar to the pattern observed when there are impurities present in the system [9].

An interesting feature here, and a crucial difference to the case of "real" impurities, is that only a fraction of the step shows oscillations and that the number of affected steps is limited. The oscillating fraction of the step decreases with increasing mode number and finally reaches zero. The reason for the oscillation cutoff is the condition that the final state of the transition, mode  $n+1$ , must be nonpropagating, which is expressed through the step functions in Eq. (8). The fraction  $\Delta$  of the step, which shows oscillations, is given by the following expression

$$\Delta = \frac{1 - \Omega(n + 1/2)}{1 + \Omega}, \quad (11)$$

which shows how  $\Delta$  depends on mode number and frequency. It is also seen in Fig. 3 that the amplitude of the oscillations increases with step number. This is expected from the way the photoconductance depends on the mode number, see Eq. (8). Another feature is that the period of the oscillations increases with the microconstriction width, which is understood by noting that the phase  $\phi$  is roughly proportional to the square root of  $d$ .

Concerning the possibilities to experimentally verify our predictions, there are two possible mechanisms that could destroy the interference effect; temperature smearing of the Fermi distribution function and relaxation of

the electrons leading to excitation of phonons. For the temperature smearing our estimate is that the temperature  $T$  must satisfy  $T \ll T_F \delta_0 / (k_F d)^2$ , where  $\delta_0$  is the period—in units of  $(k_F d)^2$ —of the conductance oscillation (cf. Fig. 3). The strongest restriction is found at the first conductance step of Fig. 3(c), which gives the condition  $T \ll 50$  K.

As for phonon scattering, the requirement is that  $l_{ph} \gg L$  where  $l_{ph}$  is the phonon mean free path and  $L$  is the size of the microwidening. The phonon mean free path is given by  $l_{ph} = (1/g)(v_F/\omega_D)(\hbar\omega_D/E_{exc})^3$ , where  $g$  is an electron-phonon coupling constant,  $\omega_D$  is the Debye frequency,  $E_{exc}$  is the excitation energy, and  $v_F$  is the Fermi velocity. In our case we have  $E_{exc} = 0.3E_F$  and taking  $\omega_D = 10^{13}$  s<sup>-1</sup>,  $v_F = 10^5$  m/s, and  $g = 1$  we obtain the phonon mean free path  $l_{ph} = 10$   $\mu$ m. Since the length  $L$  of our microwidening, in the largest case, is taken to be 4  $\mu$ m, we believe that excitation of phonons should not destroy the interference effect. At the same time we note that the phase memory of an electron trapped in the bound state is lost, and therefore interference effects involving electrons moving out of the bound state will be washed out. In our model we have calculated interference effects as a result of electrons moving *into* the bound state, which is the only relevant process for our choice of parameters. However, if we decrease the frequency of the electromagnetic field by a factor of 10, the phonon mean free path will instead be limited by the temperature, and at low temperatures we can expect interference effects involving electrons moving out of the bound state to show up as a fine structure added to the present results.

In conclusion, we have shown that it is possible to produce a special type of quantum disorder in an initially “clean” system by applying a homogeneous electromagnetic field. An important role is played by the geometry. The electromagnetic field transforms an arbitrary geometry into a system of scatterers, where the configuration of the scatterers depends on the particular geometry in question. One reason why this method of creating disorder is appealing is that by varying the frequency of the electromagnetic field we can effectively move the position of the impurities without changing the geometry of the experiment. Our estimates of the electromagnetic field strength and frequency needed to observe the interference effect indicate that an experimental realization of our predictions is possible [10].

Another interesting aspect is that by varying the amplitude of the electromagnetic field we can vary the cross section of scattering. This opens up the exciting possibility to study the transition from weak to strong localization, which might be possible in this type of system. Even if the scattering from a single scattering center is weak we can expect a finite localization length because of the one-dimensional character of our system. Therefore we expect size effects in the electron transport, when the length of the microconstriction becomes comparable

with the localization length. Scattering from “real” impurities should not destroy the localization effect, at least not when there are only a few modes present in the system. However, there is need for a more thorough investigation in order to clarify how far the analogy with localization caused by static impurity disorder can be extended; this is still an open question.

This work was supported by the Swedish Royal Academy of Sciences (KVA) and the Natural Science Research Council (NFR). Two of us (L.G. and V.K.) acknowledge the hospitality of the Department of Applied Physics, CTH/GU. We gratefully acknowledge discussions with B. Altshuler, T. Claeson, E. Kollberg, V. Shumeiko, and O. Vendik.

---

\*Permanent address: Institute for Low Temperature Physics and Engineering, Ukrainian Academy of Sciences, 47 Lenin Avenue, 310164 Kharkov, Ukraine.

†Permanent address: Institute for Physics and Technology, Ukrainian Academy of Sciences, Kharkov, Ukraine.

- [1] B.L. Altshuler and A.G. Aronov, in *Modern Problems in Condensed Matter Science*, edited by A.L. Efros and M. Pollak (North-Holland, Amsterdam, 1985).
- [2] C.W.J. Beenakker and H. van Houten, in *Solid State Physics*, edited by H. Ehrenreich and D. Turnbull (Academic, San Diego, 1991), Vol. 44, p. 1.
- [3] A. Grincwajg, L.Y. Gorelik, V.Z. Kleiner, and R.I. Shekhter, Göteborg Report No. APR 94-1.
- [4] A. Grincwajg, M. Jonson, and R.I. Shekhter, *Phys. Rev. B* **49**, 7557 (1994).
- [5] M. Büttiker, *Phys. Rev. B* **41**, 7906 (1990).
- [6] We will consider only single-photon scattering, neglecting nonlinear effects such as Rabi oscillations [11]. This is possible since the propagating electrons spend only a short time  $t_p$  in the spatial region where the interlevel spacing  $\Delta E$  (see Fig. 1) is close (on the scale of the Rabi frequency  $\omega_R = |A_{\alpha\beta}|/\hbar$ ) to the frequency  $\omega$  of the electromagnetic field. The single-photon approximation is therefore correct if  $\omega_R t_p \ll 1$ .
- [7] Summation over the quantum numbers  $\beta$  of a bound state is to be interpreted as summations over the discrete mode number and wave vector characterizing this state and is dimensionless. Summation over the quantum numbers  $\alpha$  of a propagating state is to be interpreted as a summation over the discrete mode number and an integration over the continuous wave vector characterizing this state and has the dimension 1/length.
- [8] L.Y. Gorelik, A. Grincwajg, M. Jonson, V.Z. Kleiner, and R.I. Shekhter (unpublished).
- [9] G. Timp, R. Behringer, S. Sampere, J.E. Cunningham, and R.E. Howard, in *Proceedings of the International Symposium on Nanostructure Physics and Fabrication*, edited by W.P. Kirk and M. Reed (Academic, New York, 1989), p. 331.
- [10] Erik Kollberg (private communication).
- [11] L. Allen and J.H. Eberly, *Optical Resonances and Two-Level Atoms* (Wiley, New York, 1975).